

Note on Stability and Holographic Renyi Entropy in New Hyperbolic AdS Black Holes

Zhen Fang,^a Song He,^{b,c,a} Danning Li^a

^a*State Key Laboratory of Theoretical Physics, Institute of Theoretical Physics, Chinese Academy of Science, Beijing 100190, P. R. China*

^b*Max Planck Institute for Gravitational Physics (Albert Einstein Institute) Am Mühlenberg 1, 14476 Golm, Germany*

^c*Yukawa Institute for Theoretical Physics, Kyoto University, Kitashirakawa Oiwakecho, Sakyo-ku, Kyoto 606-8502, Japan*

E-mail: fangzhen@itp.ac.cn, hesong17@gmail.com, lidn@itp.ac.cn

ABSTRACT: We construct a series of new hyperbolic black hole solutions in Einstein-Scalar system and we apply holographic approach to investigate the spherical Renyi entropy in various deformations. Especially, we introduce various powers in the scalar potential for massive and massless scalar cases. These scalar potentials correspond to deformation of dual CFTs. We make use of a systematic way to generate numerical hyperbolic AdS black hole solutions. Based on these solutions, we study the temperature dependent condensation of dual operator of massive and massless scalar respectively. These condensations show that there might be phase transitions in deformed CFTs. We also compare free energy between hyperbolic black hole solutions and hyperbolic AdS-SW black hole to judge phase transitions. In order to confirm the existence of phase transitions, we turn on linear inhomogeneous perturbation to test stability of these hyperbolic AdS black holes. In this paper, we show how potential parameters affect the stability of hyperbolic black holes in several specific examples. For generic value of potential parameters, it needs further study to see how the transition happens. Finally, we comment on these instabilities associated with spherical Renyi entropy in dual deformed CFTs.

KEYWORDS: Hyperbolic AdS Black Hole Solutions, Stability, Holographic Renyi Entropy, AdS/CFT

Contents

1	Introduction	1
2	Gravity Setup	3
3	Asymptotic AdS Solutions	4
3.1	Massless Scalar Cases	4
3.2	Massive Scalar Cases	5
4	New Hyperbolic Black Hole Solutions	6
4.1	Massless Scalar Cases	6
4.2	Massive Scalar Cases	7
5	Energy Momentum Tensor and Free energy	7
5.1	Energy Momentum Tensor	8
5.1.1	Massless Scalar Cases	8
5.1.2	Massive Scalar Cases	10
5.2	The Difference of Free Energy	10
6	Phase Transitions	11
6.1	Condensation	11
6.1.1	Massless Cases	11
6.1.2	Massive Cases	14
7	Instability for the Normalizable Mode	18
7.1	Massless Scalar Cases	19
7.2	Massive Scalar Cases	19
8	Comments on Renyi Entropy in CFTs	21
8.1	Replica and Renyi Entropy	22
8.2	Spherical Renyi Entropy as Thermal Entropy	23
9	Conclusions and Discussions	24

1 Introduction

The stability of black holes in anti-de Sitter space has been widely studied in the context of the AdS/CFT correspondence [1][2][3][4], where they are dual to finite temperature states. Dynamical and thermodynamical stability properties provide a novel window on the phase structure of the dual CFTs. In holographic approaches to condensed matter physics the

instability of a black hole to the condensation of scalar hair is dual to a superconducting phase transition [5][6].

We will focus on the instability of hyperbolic AdS black holes and finally comment on holographic Renyi entropy. There are many hyperbolic AdS black holes, which were constructed in [7][8][9][10][11][12]. In [13], it was shown that static black holes with hyperbolic horizons can become unstable to the formation of uncharged scalar hair on the horizon of the black hole due to the presence of an extremal limit with near-horizon geometry $AdS_2 \times H^3$ [14][15][16][17]. Further, authors of [18] introduced a topological black hole with a minimal coupled scalar field of negative mass-square and showed this new stability appeared. In [19], they mapped the instability of this gravity solution to the phase transition happened in dual CFTs by holographic Renyi entropy. In [20], they investigated charged hyperbolic black holes, which became unstable to presence of scalar hair at sufficiently low temperature. Such kind of instability is the same as the holographic superconducting instability in boundary hyperbolic space. In summary, scalar fields with masses below the effective Breitenlohner-Freedman bound for the near-horizon AdS_2 will become unstable at sufficient low temperatures. This happens for charged and uncharged black holes; for AdS black holes with spherical horizons, such instabilities occur at finite chemical potential. When the mass of scalar field is below this bound, the black hole becomes unstable and will decay to a hairy black hole solution. The corresponding boundary operator acquires a non-zero expectation value.

In this paper, we have constructed a series of generic hyperbolic AdS black holes with neutral self interaction scalar. More precisely, in this system, we introduce series of specific powers of scalar in scalar potential. In [19], the authors showed that there was an instability in massive scalar hairy hyperbolic AdS black hole. The instability would induce a phase transition and entanglement Renyi entropy (ERE) also confirmed the phase transition. In our setup, we introduce higher powers of scalar self-interactions which correspond to deformation of CFTs. We start with the generic gravity setup and see what will happen. Firstly, we work out these gravity solution in UV region which will be useful to extract UV asymptotic AdS boundary condition. Finally, we can find hyperbolic AdS black hole solution numerically in various scalar potentials. In terms of that the EE for the spherical region of CFT is equivalent to the thermal entropy of the CFTs on the hyperbolic cylinder. This thermal entropy can be translated to the horizon entropy of an appropriate black hole with hyperbolic boundary. Basing on these hyperbolic AdS hairy black holes, we can make use of this dictionary to obtain the ERE in dual deformed CFTs. ERE obtained in our setup show that there are instabilities inducing phase transitions in dual CFTs. We also extract the condensation of dual operator with respect to temperature in each solution. The condensation of dual operator confirms that the phase transition might happen. To make sure of the phase transitions, we compare the free energy between the hyperbolic scalar hairy AdS black hole solutions (HSHAdS) and hyperbolic AdS-SW black hole to reveal the transition. Further, we turn on the in-homogenous linear perturbation to test the stability of HSHAdS and the stability condition highly constrains the potential parameters presented in the massive and massless scalar potential. We will give some explicit examples to show what kinds of scalar potential will give stable HSHAdS. Finally, one can make use

of the stability to obtain the phase structure of these theories roughly. In terms of that EE for the spherical region of CFT can be calculated by thermal entropy of HSHAdS, the ERE also implies the phase transition.

An overview of the remainder of the paper is as follows: in section 2, we firstly set up the gravity which is our starting point. In section 3, we will list the asymptotic AdS boundary behavior which is controlled by Einstein equations for massless and massive scalar respectively. These UV behaviors are useful to obtain the numerical solutions. In section 4, we show various new hyperbolic scalar hairy AdS black hole solutions. In section 5, we study the boundary energy momentum tensor of these solutions with introducing various of boundary counter terms in massless and massive scalars respectively. Further, we evaluate the free energy of these solutions. In section 6, through above numerical analysis, we found that there are interesting phase transitions in deformed CFTs. We make use of condensation of dual operators and free energy of each solution to confirm phase transition will really happen in deformed CFTs. In section 6, we have demonstrated that the hyperbolic black holes are unstable and Renyi entropies show a phase transition. Therefore, in section 7, we turn to the physical case of these models which are normalizable on hyperboloid. In section 8, we will devote to conclusions and discussions.

2 Gravity Setup

The gravity action in 5D spacetime in Einstein frame is

$$S_{5D} = \frac{1}{16\pi G_5} \int d^5x \sqrt{-g} \left(R - \frac{4}{3} \partial_\mu \phi \partial^\mu \phi - V(\phi) \right). \quad (2.1)$$

Here G_5 is the 5D Newton constant, g is the 5D metric determinant and ϕ, V are the scalar field and the corresponding potential. The equations of motion are

$$E_{\mu\nu} + \frac{1}{2} g_{\mu\nu} \left(\frac{4}{3} \partial_\mu \phi \partial^\mu \phi + V(\phi) \right) - \frac{4}{3} \partial_\mu \phi \partial_\nu \phi = 0, \quad (2.2)$$

where $E_{\mu\nu} = R_{\mu\nu} - \frac{1}{2} R g_{\mu\nu}$ is Einstein tensor.

We would like to choose the following ansatz to solve the Einstein equations of motion,

$$\begin{aligned} ds^2 &= -\frac{L^2 e^{2A_e(z)}}{z^2} \left(-f(z) dt^2 + \frac{1}{f(z)} dz^2 + (d\psi^2 + \sinh^2(\psi) d\theta^2 + \sin^2(\theta) \sinh^2(\psi) d\varphi^2) \right) \\ &= -\frac{L^2 e^{2A_e(z)}}{z^2} \left(-f(z) dt^2 + \frac{1}{f(z)} dz^2 + dH^3 \right), \end{aligned} \quad (2.3)$$

where H^3 is 3 dimensional hyperbolic space and L is AdS radius. In terms of the above ansatz, one can obtain equations,

$$\begin{aligned} A_e''(z) - A_e'(z)^2 + \frac{2A_e'(z)}{z} + \frac{4}{9} \phi'(z)^2 &= 0, \\ f''(z) + f'(z) \left(3A_e'(z) - \frac{3}{z} \right) - \frac{4}{L^2} &= 0, \\ \phi''(z) + \left(3A_e'(z) + \frac{f'(z)}{f(z)} - \frac{3}{z} \right) \phi'(z) - \frac{3L^2 e^{2A_e(z)} V'(\phi(z))}{8z^2 f(z)} &= 0. \end{aligned} \quad (2.4)$$

One more constrain equation is

$$6A'_e(z)^2 + \left(\frac{3f'(z)}{2f(z)} - \frac{12}{z} \right) A'_e(z) + \frac{L^2 e^{2A_e(z)} V(\phi(z))}{2z^2 f(z)} - \frac{3f'(z)}{2zf(z)} + \frac{3}{L^2 f(z)} + \frac{6}{z^2} - \frac{2}{3} \phi'(z)^2 = 0 \quad (2.5)$$

(2.5) is not independent on the other three equations in (2.4). Once the gravity solution is obtained from (2.4), one could use (2.5) to check the solution.

Here, we note that (2.4) would impose a natural boundary condition near horizon. If one collects all the terms with a denominator $f(z)$, the results are as following

$$\frac{Q(z)}{8z^2 f(z)} \quad (2.6)$$

with $Q(z) \equiv 8z^2 f' \phi' - 3L^2 e^{2A_e} V'(\phi)$. Since the horizon is not a real singularity, the apparent singularity $f(z_h) = 0$ in Eq.(2.4) should be canceled by requiring $Q(z_h) = 0$. Later, we will try to solve this boundary value problem using numerical method developed in Ref.[21].

3 Asymptotic AdS Solutions

Based on the set up in previous sections, we pay attention to how to solve the whole system in the UV region $z \sim 0$ in this section. Near the UV region, we can use series expansion to find the solution of unknown function in metric ansatz (2.3). These expansions will be helpful to the later numerically computation to show the full numerical solutions.

3.1 Massless Scalar Cases

In this section, we will try to find the UV expansion of gravity solution with massless scalar with potential like

$$V = \frac{1}{L^2} \left(-12 + v_3 \phi^3 + v_4 \phi^4 + v_6 \phi^6 \right) \quad (3.1)$$

In this potential, we set the mass of the scalar to be zero and call this case by massless scalar case for convenience in this paper.

Firstly, the UV behavior of the black hole should be asymptotical AdS and there is a horizon parameterized by z_h in the IR region. We find an algorithm to get the numerical solution consistently. Roughly speaking, we try to expand in power series all unknown functions as positive powers of z . The UV solution can be expressed by following form

$$\begin{aligned} \phi(z) = & p_4 z^4 + \frac{2p_4 z^6}{3L^2} + \frac{z^8 (p_4 - f_4 L^4 p_4)}{2L^4} - \frac{2p_4 z^{10} (2f_4 L^4 - 1)}{5L^6} \\ & + \frac{z^{12} (1728f_4^2 L^8 p_4 - 5184f_4 L^4 p_4 + 81L^8 p_4^3 v_4 + 512L^8 p_4^3 + 1728p_4)}{5184L^8} \\ & + \frac{z^{14}}{997920L^{10}} \left(855360f_4^2 L^8 p_4 - 1140480f_4 L^4 p_4 + 34749L^8 p_4^3 v_4 \right. \\ & \left. + 217600L^8 p_4^3 + 285120p_4 \right) + O(z^{16}) \end{aligned} \quad (3.2)$$

$$\begin{aligned}
A_e(z) = & \frac{1}{81}(-8)p_4^2 z^8 - \frac{64p_4^2 z^{10}}{495L^2} + \frac{64p_4^2 z^{14}(3f_4 L^4 - 2)}{945L^6} + \frac{16z^{12}(2f_4 L^4 p_4^2 - 3p_4^2)}{351L^4} \\
& + \frac{z^{16}(-69984f_4^2 L^8 p_4^2 + 279936f_4 L^4 p_4^2 - 2187L^8 p_4^4 v_4 - 11776L^8 p_4^4 - 116640p_4^2)}{892296L^8} \\
& - \frac{2z^{18}(285120f_4^2 L^8 p_4^2 - 475200f_4 L^4 p_4^2 + 8019L^8 p_4^4 v_4 + 43520L^8 p_4^4 + 142560p_4^2)}{2285415L^{10}} + O(z^{20})
\end{aligned} \tag{3.3}$$

$$\begin{aligned}
f(z) = & 1 - \frac{z^2}{L^2} + \frac{32p_4^2 z^{14}(74f_4 L^4 - 33)}{15015L^6} + f_4 z^4 - \frac{32p_4^2 z^{10}}{405L^2} \\
& + \frac{8z^{12}(11f_4 L^4 p_4^2 - 9p_4^2)}{891L^4} - \frac{8z^{16}(15f_4^2 L^8 p_4^2 - 42f_4 L^4 p_4^2 + 13p_4^2)}{1755L^8} \\
& + \frac{z^{18}(-645408f_4^2 L^8 p_4^2 + 819072f_4 L^4 p_4^2 - 3645L^8 p_4^4 v_4 - 48640L^8 p_4^4 - 194400p_4^2)}{3903795L^{10}} + O(z^{20})
\end{aligned} \tag{3.4}$$

One can find the black hole solution in the UV region can be expressed in series of powers of z . In principle, one can obtain more higher powers of z to get the full expression of black hole background. Unfortunately, we can not obtain closed form of the black hole solution. The main reason is that we do not find simple recurrence relation among the coefficients of each power of z , as explained in [21]. In terms of AdS/CFT dictionary, the massless neutral scalar in the bulk will dual to $\Delta = 4$ operator in field theory side. p_4 is the expectation value of dual operator. It is easy to see that the black hole solution with asymptotical AdS can be controlled by integral constants p_4, f_4 in (3.2)(3.3)(3.4). p_4, f_4 are determined by boundary condition in IR region. Here we choose parameters p_4, f_4 to show one black hole solution numerically. Here p_4, f_4 are not independent and they are related to the horizon position z_h such that $Q(z_h) = 0$. We impose $\phi(z_h)$ to be regular, which could be guaranteed by requiring $Q(z_h) = 0$.

3.2 Massive Scalar Cases

Firstly, we try to figure out asymptotic AdS solution of our setup with potential like

$$V = \frac{1}{L^2} \left(-12 - \frac{16\phi^2}{3} + v_3\phi^3 + v_4\phi^4 + v_6\phi^6 \right) \tag{3.5}$$

In this potential, we have introduced a mass term of scalar field and we will call this case by massive scalar case. With above potential, we can find the solution near the UV region analytically. As shown in massless case, the UV behavior of the black hole should be asymptotical AdS and there is a horizon in the IR region which is parameterized by z_h .

The asymptotic solution is following

$$\begin{aligned}
\phi(z) = & p_2 z^2 + p_{22} z^2 \log(z) + \frac{1}{64} z^4 (18 p_2^2 v_3 - 36 p_{22} p_2 v_3 + 27 p_{22}^2 v_3 + 32 p_{22}) + \frac{9}{32} p_{22}^2 v_3 z^4 \log^2(z) \\
& + \frac{9}{16} z^4 (p_2 p_{22} v_3 - p_{22}^2 v_3) \log(z) + O(z^6 \log(z)) \\
& - \frac{z^6}{18432000 L^4} (4608000 f_4 L^4 p_2 + 2304000 f_4 L^4 p_{22} - 729000 L^4 p_2^3 v_3^2 \\
& + 1366875 L^4 p_{22}^3 v_3^2 - 3371625 L^4 p_2 p_{22}^2 v_3^2 + 2551500 L^4 p_2^2 p_{22} v_3^2 - 1728000 L^4 p_2^3 v_4 \\
& + 648000 L^4 p_{22}^3 v_4 - 1944000 L^4 p_2 p_{22}^2 v_4 + 2592000 L^4 p_2^2 p_{22} v_4 - 3276800 L^4 p_2^3 \\
& + 595968 L^4 p_{22}^3 - 2043904 L^4 p_2 p_{22}^2 + 2129920 L^4 p_2^2 p_{22} - 2592000 L^2 p_2^2 v_3 \\
& - 1620000 L^2 p_{22}^2 v_3 + 2592000 L^2 p_2 p_{22} v_3 - 4608000 p_{22}) + O(z^8) \tag{3.6}
\end{aligned}$$

$$\begin{aligned}
A_e(z) = & \frac{z^6 (-74088 p_2^3 v_3 + 142884 p_{22} p_2^2 v_3 - 96390 p_{22}^2 p_2 v_3 - 14013 p_{22}^3 v_3 - 131712 p_{22} p_2 - 25088 p_{22}^2)}{1555848} \\
& - \frac{1}{21} p_{22}^3 v_3 z^6 \log^3(z) + \frac{1}{98} z^6 (9 p_{22}^3 v_3 - 14 p_2 p_{22}^2 v_3) \log^2(z) \\
& + \frac{z^6 (-2295 p_{22}^3 v_3 + 6804 p_2 p_{22}^2 v_3 - 5292 p_2^2 p_{22} v_3 - 3136 p_{22}^2) \log(z)}{37044} \\
& + \frac{(-200 p_2^2 - 20 p_{22} p_2 - 21 p_{22}^2) z^4}{2250} - \frac{4}{45} p_{22}^2 z^4 \log^2(z) - \frac{2}{225} (p_{22}^2 + 20 p_2 p_{22}) z^4 \log(z) + O(z^6) \tag{3.7}
\end{aligned}$$

$$\begin{aligned}
f(z) = & 1 - z^2 f_4 z^4 - \frac{2 (900 p_2^2 - 660 p_{22} p_2 + 407 p_{22}^2) z^6}{10125} \\
& - \frac{1}{45} 8 p_{22}^2 z^6 \log^2(z) - \frac{8}{675} (30 p_2 p_{22} - 11 p_{22}^2) z^6 \log(z) + O(z^8) \tag{3.8}
\end{aligned}$$

It is easy to see that the black hole solution with asymptotical AdS can be controlled by three integral constants p_2, p_{22}, f_4 . p_2, p_{22}, f_4 are determined by boundary condition in IR region. In this case, p_2, p_{22}, f_4 are not independent and they are determined by the black hole horizon z_h . We still impose $\phi(z_h)$ to be regular which is horizon boundary condition. The temperature is also defined by $T = \frac{f'(z)}{4\pi} |_{z=z_h}$.

4 New Hyperbolic Black Hole Solutions

In this paper, we focus on the scalar potential with polynomial form of scalar with highest sextic self-interaction. We explore a systematic way to generate fully backreaction gravity solutions and investigate corresponding phase structure. In the following subsections, we will show two examples to demonstrate these configurations of fields.

4.1 Massless Scalar Cases

In this subsection, we numerically solve the gravity setup with generic potential like $V(\phi) = \frac{1}{L^2} (-12 + v_4 \phi^4)$. Here we just set the mass term of scalar to be vanishing. In this case, the

dual operator O_1 is relate to dimension 4 glueball operator. One can check that the solution satisfies asymptotical AdS UV boundary condition. In Fig.1(a)(b)(c), the UV behavior of these fields has been shown respectively. We just solve these solutions from UV to IR. In the IR, we should impose regular boundary conditions to all these fields. Especially, we have shown $f(z_h) = 0$ numerically in Fig. 1(c), where $Q(z)$ has been defined in Sec.2 to check IR boundary condition. In this example shown in Fig.1(a)(b)(c), we can turn off the potential parameter v_4 and reproduce the case studied in [19]. For case $v_4 = 0$, the condensation of dual operator and free energy will be also studied in section 6.1.1 which is consistent with studies in [19].

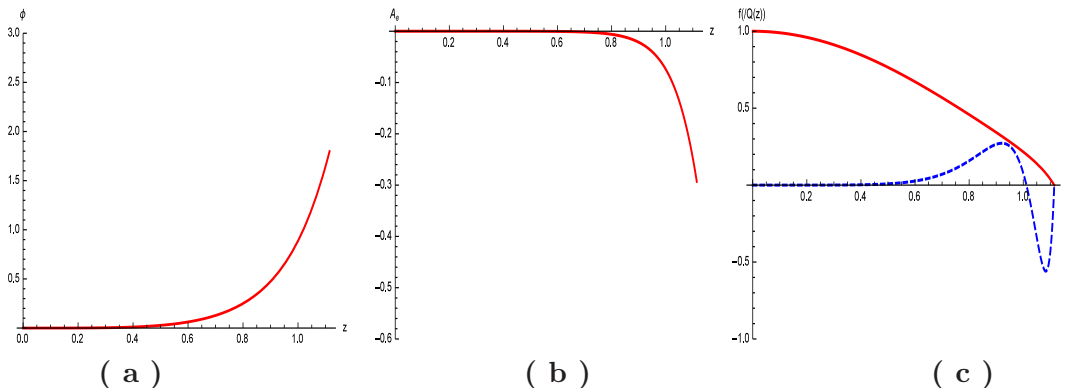


Figure 1. Characteristic solutions when $V(\phi) = -\frac{12}{L^2} + \frac{\nu_4 \phi^4}{L^2}$ with $\nu_4 = -8$. To get these solutions, we have taken $f_4 = 0.2445, p_2 = 0.36734\dots$. In Panel.(a) and Panel.(b), the solutions of ϕ and A_e are given. In Panel.(c), the solutions of f is shown in red solid line, while the corresponding $Q(z)$ is shown in blue dashed line(Here, in order to put the two in the same figures, we plot $Q(z)/50$, which is zero at the same z as $Q(z)$).

4.2 Massive Scalar Cases

In this subsection, we numerically solve the gravity setup with potential like $V(\phi) = \frac{1}{L^2} (-12 - \frac{16}{3}\phi^2 + \nu_4\phi^4)$. Here we set the mass of scalar to be $m^2 = -\frac{16}{3L^2}$ which corresponds to dimension-2 operators in 4D. In terms of AdS dictionary, the dual operator O_2 is related to meson operator. In this case, one have set $p_{22} = 0$ to find solution and the p_{22} corresponds to source of dual operator O_2 in terms of AdS/CFT. In Fig. 2(a)(b)(c), we show the expected IR and UV behaviors of all related fields in Einstein equations. Once we obtain these non trivial configurations, we can go further to study their stability and ERE in dual field theories.

5 Energy Momentum Tensor and Free energy

In this section, we turn to study the stability of hyperbolic AdS black hole solutions. Firstly, to obtain well defined energy momentum tensor on the boundary, one should introduce the suitable counter terms. For later use, we will work out a well defined counter term for these

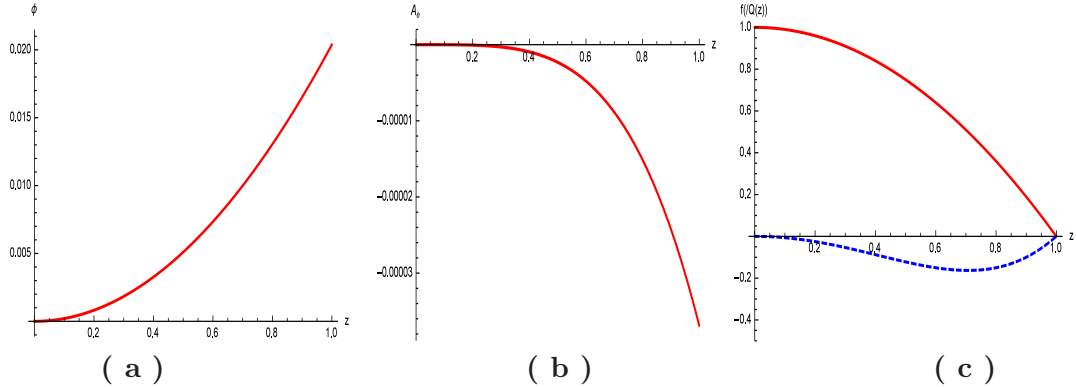


Figure 2. Characteristic solutions when $V(\phi) = -\frac{12}{L^2} - \frac{16\phi^2}{3L^2} + \frac{\nu_4\phi^4}{L^2}$ with $\nu_4 = -8$. To get these solutions, we have taken $p_{22} = 0, f_4 = -0.001, p_2 = 0.0203818\dots$. In Panel.(a) and Panel.(b), the solutions of ϕ and A_e are given. In Panel.(c), the solutions of f is shown in red solid line, while the corresponding $Q(z)$ is shown in blue dashed line.

gravity solutions and these terms will be also used in studying free energy and spherical Renyi entropy of dual CFTs.

5.1 Energy Momentum Tensor

In this subsection, we would like to introduce the counter terms to cancel the UV divergences of the action and make the energy momentum tensor of dual field theory well defined. We just introduce generic gauge invariant counter terms with undetermined coefficients in our system. Finally, we can solve these coefficients to cancel the divergences in massless and massive cases respectively in this paper.

5.1.1 Massless Scalar Cases

For massless scalar case, the total action now becomes

$$\begin{aligned}
 I_{\text{ren}} &= S_{5\text{D}} + S_{\text{GH}} + S_{\text{count}} \\
 &= \frac{1}{16\pi G_5} \int_M d^5x \sqrt{-g} \left(R - \frac{4}{3} \partial_\mu \phi \partial^\mu \phi - V_E(\phi) \right) \\
 &\quad - \frac{1}{16\pi G_5} \int_{\partial M} d^4x \sqrt{-\gamma} \left[2K - \frac{6}{L} + \lambda_1 \mathcal{R} + \lambda_2 \mathcal{R}_{ab} \mathcal{R}^{ab} + \lambda_3 \mathcal{R}^2 + \dots \right],
 \end{aligned} \tag{5.1}$$

with $\lambda_1, \lambda_2, \lambda_3$ undermined coefficients of counter terms [22][23][24][25][26][27] $\mathcal{R}, \mathcal{R}_{ab} \mathcal{R}^{ab}, \mathcal{R}^2$ to be worked out later. The first term of the last line in (5.1) is Gibbons-Hawking term S_{GH} and the remain terms are S_{count} related to cosmological constant and scalar field. These coefficients can be fixed by canceling the divergences of boundary momentum tensor. Here K_{ij} and K are respectively the extrinsic curvature and its trace of the boundary ∂M , γ_{ij}

is the induced metric on the boundary ∂M . These quantities are defined as follows

$$\gamma_{\mu\nu} = g_{\mu\nu} + n_\mu n_\nu, \quad (5.2)$$

$$K_{\mu\nu} = h_\nu^\lambda D_\lambda n_\mu, \quad (5.3)$$

$$\gamma = \det(\gamma_{\mu\nu}), \quad (5.4)$$

$$K = g^{\mu\nu} K_{\mu\nu}, \quad (5.5)$$

where $\gamma_{\mu\nu}$ denotes the induced metric, n_μ stands for the normal direction to the boundary surface ∂M as well as D_λ stands for covariant derivative. Finally, \mathcal{R} and \mathcal{R}_{ab} are the Ricci scalar and Ricci tensor for the boundary metric respectively. In generic cases, one should introduce higher powers of \mathcal{R} and various combination of \mathcal{R}_{ab} to cancel the total UV divergence. For massive and massless cases in this paper, we just only introduce \mathcal{R} to cancel all the UV divergence. That means we can set λ_2, λ_3 to be vanishing.

In the asymptotical AdS hyperbolic black hole, the boundary surface locates at $z = 0$ surface, and usually one has to regularized it to a finite $z = \epsilon$ surface. So we have the normalized normal vector $n_\mu = \frac{\delta_z^\mu}{\sqrt{g_{zz}}}$.

To regulate the theory, we restrict to the region $z \geq \epsilon$ and the surface term is evaluated at $z = \epsilon$. The induced metric is $\gamma_{ij} = \frac{\tilde{L}^2}{\epsilon^2} g_{ij}(x, \epsilon)$, where the leading term of expansion of $g_{ij}(x, \epsilon)$ with respect to ϵ is the flat metric $g_{(0)}^{ij}$. Then the one point function of stress-energy tensor of the dual CFT is given by [28][29][30][31]

$$T_{ij} = \frac{2}{\sqrt{-\det g_{(0)}}} \frac{\delta I_{ren}}{\delta g_{(0)}^{ij}} = \lim_{\epsilon \rightarrow 0} \left(\frac{L^2}{\epsilon^2} \frac{2}{\sqrt{-\gamma}} \frac{\delta I_{ren}}{\delta \gamma^{ij}} \right). \quad (5.6)$$

The finite part of boundary energy-stress tensor is from the $O(\epsilon^2)$ of the Brown-York tensor T_{ij} on the boundary $z = \epsilon$, with

$$\begin{aligned} T_{ij} = & -\frac{1}{16\pi G_5} \left[K_{ij} - \left(K + \frac{d-2}{L} \right) g_{ij} - \lambda_1 \mathcal{R}_{ij} - 2\lambda_2 \mathcal{R}_{ik} \mathcal{R}_{jk} + \frac{\lambda_1}{2} g_{ij} \mathcal{R} - 2\lambda_3 \mathcal{R}_{ij} \mathcal{R} \right. \\ & + \frac{1}{2} \lambda_3 g_{ij} \mathcal{R}^2 - 2\lambda_2 \mathcal{R}^{kl} \mathcal{R}_{ikjl} + \lambda_2 \mathcal{R}_j^k \mathcal{R}_{il}^{kl} + \lambda_2 \mathcal{R}_i^k \mathcal{R}_{jl}^{kl} + \frac{\lambda_2}{2} g_{ij} \mathcal{R}_{kl}^{km} \mathcal{R}_{ln}^{mn} \\ & \left. + (2\lambda_3 + \lambda_2) \nabla_j \nabla_i \mathcal{R} - \lambda_2 \mathcal{R}_{ij;k}^k - (2\lambda_3 + \frac{1}{2} \lambda_2) g_{ij} \mathcal{R}_{kl;m}^{kl;m} \right], \quad (5.7) \end{aligned}$$

In the massless scalar hair hyperbolic AdS black hole, the coefficients of counter terms can be following

$$\begin{aligned} \lambda_1 &= \frac{1}{2}, \\ \lambda_2 &= 0, \\ \lambda_3 &= 0, \end{aligned} \quad (5.8)$$

where we have fixed these coefficients by removing the UV divergence $z \rightarrow 0$ appeared in on-shell action of massless scalar. Directly evaluate (5.7) using (5.6), we get

$$T_{tt} = \frac{1}{16\pi G} \left(\frac{3L}{8} - \frac{3f_4 L}{2} \right). \quad (5.9)$$

5.1.2 Massive Scalar Cases

For massive scalar, the total action will be different from massless cases. The main reason is that the UV behavior of massive scalar is different from the massless cases. The divergences in the UV region are very sensitive to UV behavior. In massive case, we will introduce following counter term to cook up well defined on-shell action.

$$\begin{aligned}
I_{\text{ren}} &= S_{5\text{D}} + S_{\text{GH}} + S_{\text{count}} \\
&= \frac{1}{16\pi G_5} \int_M d^5x \sqrt{-g} \left(R - \frac{4}{3} \partial_\mu \phi \partial^\mu \phi - V_E(\phi) \right) \\
&\quad - \frac{1}{16\pi G_5} \int_{\partial M} d^4x \sqrt{-\gamma} \left[2K - \frac{6}{L} + \lambda_{m1} \mathcal{R} + \lambda_{m2} \phi^2 + \lambda_{m3} \phi \mathcal{R} + \dots \right],
\end{aligned} \tag{5.10}$$

In terms of (5.6), the boundary energy momentum tensor would be

$$T_{ij} = \frac{1}{16\pi G} \left[K_{ij} - \left(K + \frac{d-2}{2} - \lambda_{m2} \phi^2 \right) g_{ij} + (\lambda_{m3} \phi + \lambda_{m1}) (\mathcal{R}_{ij} - \frac{1}{2} g_{ij} \mathcal{R}) \right] \tag{5.11}$$

In the massive scalar hair hyperbolic AdS black hole, the coefficients of count terms can be following

$$\begin{aligned}
\lambda_{m1} &= \frac{1}{2}, \\
\lambda_{m2} &= \frac{8}{3}, \\
\lambda_{m3} &= \frac{2\langle O_2 \rangle}{9},
\end{aligned} \tag{5.12}$$

where $\langle O_2 \rangle$ corresponds to expectation value of dual operator O_2 of massive scalar ϕ . We have fixed these coefficients by removing the UV divergence $z \rightarrow 0$ appearing in on-shell action of massive scalar.

Directly evaluate (5.7) using (5.6), we get

$$T_{tt} = \frac{1}{16\pi G} \left(-\frac{3f_4 L}{2L^2} - \frac{\langle O_2 \rangle^2 L}{6} + \frac{3L}{8} \right). \tag{5.13}$$

5.2 The Difference of Free Energy

After introducing the counter term to remove the divergence of the action, we can work out the on shell action which will be helpful to test the holographic phase structures. Later, we will also make use of condensation of dual operator to get the flavor of phase transitions.

For massless scalar case, the on shell action can be

$$S_{5\text{D-BH}} = \frac{1}{16\pi G} \left(\frac{3}{4} - f_4 \right) \tag{5.14}$$

For massive scalar case, the on shell action can be

$$S_{5\text{D-BH}} = \frac{1}{16\pi G} \left(\frac{3}{4} - f_4 - \frac{1}{45} 8p_2^2 - \frac{28p_{22}p_2}{75} - \frac{416p_{22}^2}{1125} \right) \tag{5.15}$$

where we have to turn off the the source p_{22} to obtain the expectation value of dual operator in vacuum for later use.

6 Phase Transitions

In the proceeding section, we would like to study the stability of these hyperbolic AdS black hole solutions by calculating condensation of dual operator and free energy. We will show temperature dependence behaviors of condensation of operators O_1, O_2 dual to massless and massive scalar respectively. Firstly, we will make use of free energy to study the stability of these new hyperbolic black hole solutions. In this section, we mainly focus on the constant modes in which we do not turn on the in-homogenous perturbation of these solutions. The constant mode means that the field configurations only depend on holographic direction z . We should say this analysis is not so solid and later we will turn to go further to check the stability of these solutions. In section 7, we will go back to the phase structures in these theories studied in this section in terms of linear perturbation.

6.1 Condensation

In this subsection, we will figure out all fields configurations and extract the condensation of dual operator O of scalar field to see what will happen with changing related parameters, for example, temperature and coupling constant of scalar self-interaction. Basically, one can extract the condensation of dual operator by UV expansion of massless and massive scalar shown in Eq.(3.2) Eq.(3.6) in terms of AdS/CFT dictionary. The condensation will imply whether there is phase transition or not. Later, we will use free energy to confirm these phase transitions and determine the transition temperature.

6.1.1 Massless Cases

We would like to introduce several deformations in massless scalar potential, for example, adding ϕ^3, ϕ^4, ϕ^6 terms to the potential. We mainly focus on obtaining condensation of the dual $\Delta = 4$ glueball operator O_1 with respect to temperature. We will see there exist phase transition in various deformations and how these deformations affect the phase transition in details.

Firstly, we would like to calculate the condensation in massless scalar with potential like $V(\phi) = -\frac{12}{L^2} + \frac{\nu_4 \phi^4}{L^2}$. In fig.3(a), we have shown the condensation as a function of temperature. The different colored curves correspond to choose model parameter ν_4 . With increasing ν_4 , the condensation at same temperature will increase gradually. There is a transition temperature which is determined by that the condensation goes to zero. For each colored curve, the condensation is double valued function with respect to temperature from zero temperature to maximal temperature T_{max} . In fig.3(b), we calculate free energy with respect to temperature and it shows that the dashed line part is unstable comparing with solid curve. That means the T_{max} is phase transition temperature T_c in terms of free energy. Below the transition temperature T_c , the condensation is a monodrome function of temperature. At the transition temperature, the condensation will jump from finite positive value to zero and the massless hairy black hole solution is unstable comparing with hyperbolic AdS-SW black hole. That is to say hyperbolic AdS-SW black hole is favored when $T \geq T_c$. Up to this stage, we find the instability exists in this case.

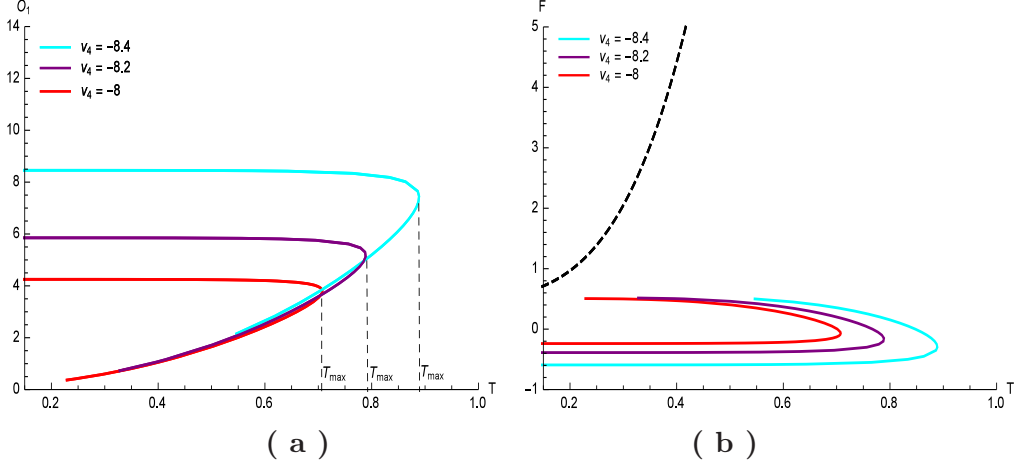


Figure 3. The condensation is as a function of temperature in massless scalar case with potential $V(\phi) = -\frac{12}{L^2} + \frac{\nu_4\phi^4}{L^2}$.

Secondly, we would like to calculate the condensation O_1 in massless scalar with potential like $V(\phi) = -\frac{12}{L^2} + \frac{\nu_4\phi^4}{L^2} + \frac{\nu_6\phi^6}{L^2}$. In fig.4(a), we have shown the condensation as a function of temperature. The different colored curves correspond to choose different model parameter ν_6 with fixing ν_4 . With increasing ν_6 , the condensation at same temperature will decrease gradually. There is a transition temperature which is determined by that the condensation goes to zero. For each colored curve, the condensation is double valued function with respect to temperature from zero temperature to maximal temperature T_{max} . In fig.4(b), we calculate free energy with respect to temperature and it shows that the dashed line part is unstable comparing with solid curve in $T < T_{max}$. That means the T_{max} is phase transition temperature T_c . Below the transition temperature T_c , the condensation is a monodrome function of temperature. At the transition temperature, the condensation will jump from finite positive value to zero and the massless hairy black hole solution is unstable comparing with hyperbolic AdS-SW black hole in $T > T_{max}$. That is also to say hyperbolic AdS-SW black hole is favored when $T \geq T_c$. Below the transition temperature, the condensation is a monodrome function of temperature. At the transition temperature, the condensation will jump from finite positive value to zero. We can see that $\frac{\nu_6\phi^6}{L^2}$ does not change the type of phase transition induced by $\frac{\nu_4\phi^4}{L^2}$.

Finally, we would like to calculate the condensation in massless scalar with potential like $V(\phi) = -\frac{12}{L^2} + \frac{\nu_3\phi^3}{L^2} + \frac{\nu_4\phi^4}{L^2}$. In fig.5(a), the condensation as a function of temperature has been presented. The different colored curves correspond to choose model parameter ν_3 with fixing ν_4 . With increasing ν_3 , the condensation at same temperature will decrease gradually. For each colored curve, the condensation is double valued function with respect to temperature from zero temperature to maximal temperature T_{max} . In fig.5(b), we also calculate free energy with respect to temperature and it shows that the dashed line part is unstable comparing with solid curve. That means the T_{max} is still phase transition temperature T_c in this case. Below the transition temperature T_c , the condensation is a

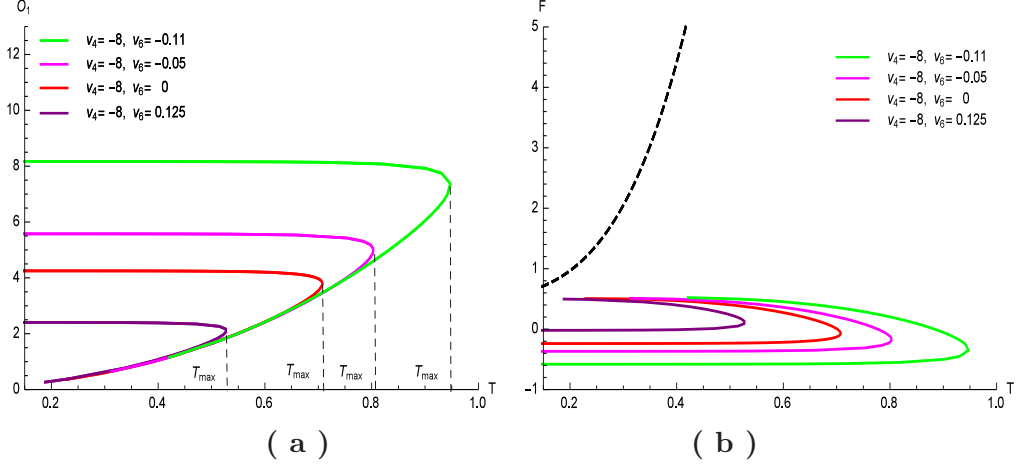


Figure 4. The condensation is as a function of temperature in massless scalar case with potential $V(\phi) = -\frac{12}{L^2} + \frac{\nu_6 \phi^6}{L^2}$.

monodrome function of temperature. At the transition temperature, the condensation will jump from finite positive value to zero and the massless hairy black hole solution is unstable comparing with hyperbolic AdS-SW black hole. That is to say hyperbolic AdS-SW black hole is favored when $T \geq T_c$. Below the transition temperature, the condensation is a monodrome function of temperature. At the transition temperature, the condensation will jump from finite positive value to zero. The deformation from $\frac{\nu_3 \phi^3}{L^2}$ does not change the type of phase transition induced by $\frac{\nu_4 \phi^4}{L^2}$ qualitatively.

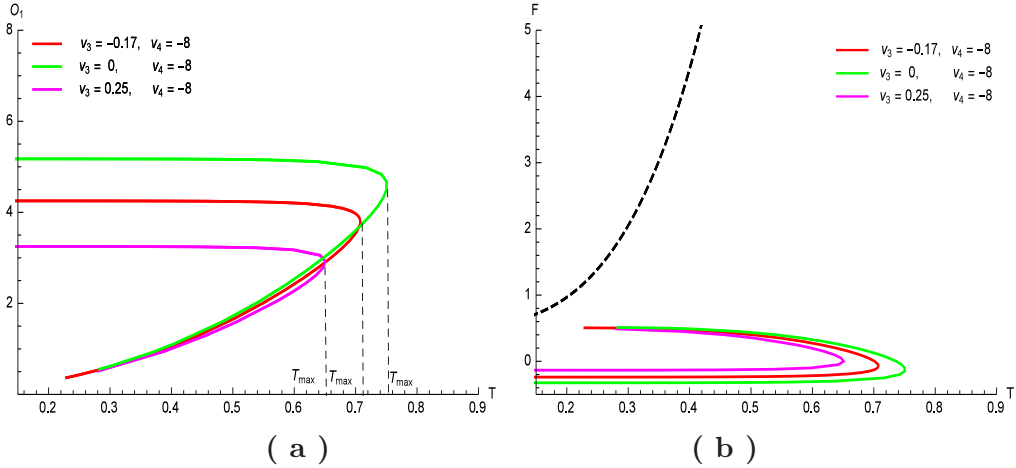


Figure 5. The condensation is as a function of temperature in massless scalar case with potential $V(\phi) = -\frac{12}{L^2} + \frac{\nu_3 \phi^3}{L^2} + \frac{\nu_4 \phi^4}{L^2}$.

In summary, we introduce three types special deformations like ϕ^3, ϕ^4, ϕ^6 in massless neutral scalar potential in the bulk. We calculate the condensation of dual operator of the scalar with respect to temperature. We find that there are phase transitions in deformed

theories. We calculate the condensation as a function of temperature numerically and find the transition temperature. Further, we calculate the free energy to confirm the phase transitions. Finally, these phase transitions induced by three kinds of deformation are the same type qualitatively. Therefore, one can naturally expect that there are still same types of phase transitions in those cases with deformation like superposition of these three kinds of deformations. We will turn to be more rigid in section 7 to check the stability of these solutions in the low temperature region $T < T_c$. In section 7, one can find that all these massless hyperbolic hairy AdS black hole are not stable. There exist more stabler solutions, which are in-homogenous solutions. Therefore, the phase transition mentioned in this section will break down and new phase structures will emerge.

6.1.2 Massive Cases

In this subsection, we would like to deform massive scalar potential by adding ϕ^3, ϕ^4, ϕ^6 terms. We mainly focus on obtaining condensation of the dual $\Delta = 2$ operator O_2 with respect to temperature. We expect that the phase structures may be changed due to choose different operator as an order parameter. We will see there exist phase transition in various deformations and how these deformations affect the phase transition order in details.

Firstly, we will turn to study the condensation in massive scalar with potential like $V(\phi) = -\frac{12}{L^2} - \frac{16\phi^2}{3L^2} + \frac{\nu_4\phi^4}{L^2}$. In Fig.6(a), we have shown the condensation of dual operator as a function of temperature in several cases. Each case corresponds to set different values of self-interaction coupling constants ν_4 . In each case, there is a transition point when the condensation goes to vanishing. That means the mass hair AdS hyperbolic black hole is more stable than vanishing condensation solution which is hyperbolic AdS-SW black hole in low temperature region. It implies that there should be a phase transition with increasing temperature in this system. Furthermore, the types of phase transition will be changed with increasing ν_4 , which shows that the $\frac{\nu_4\phi^4}{L^2}$ deformation will play an important role to determine the transition types. In Fig.6, we increase $\nu_4 = -0.2, 0.0, 1.0$ gradually and find that transition temperature is independent on ν_4 . Furthermore, there exists a critical value for ν_{4c} between $\nu_4 = -1$ and $\nu_4 = -0.2$. Crossing this critical point, the phase transition order will be changed in $\nu_4 < \nu_{4c}$. In fig. 6(b), the free energy will increase with temperature. All colored curves will converge to a one point which corresponds to transition temperature in $\nu_4 > \nu_{4c}$. The transition temperature is the same as transition temperature given by fig. 6(a). The black dashed line in Fig. 6(b) corresponds to free energy in hyperbolic AdS-SW black hole. In Fig. 6(b), the dominate phase should be hyperbolic AdS-SW black hole above the transition temperature. The free energy can continuously converge to the transition point in Fig. 6(b) with $\nu_4 > \nu_{4c}$. But free energy will jump to the transition point with $\nu_4 < \nu_{4c}$. That is also means the order of phase transition should change suddenly and the transition temperature will be T_{max} , for example, curves shown in $\nu_4 = -1.4, -1.2, -1.0$. This phenomenon is also consistent with a condensation jump from finite value to vanishing in Fig. 6(a).

Now we will turn to study the condensation in massive scalar with potential like $V(\phi) = -\frac{12}{L^2} - \frac{16\phi^2}{3L^2} + \frac{\nu_6\phi^6}{L^2}$. We introduce $\frac{\nu_6\phi^6}{L^2}$ deformation and to see what will happen for phase transition. In Fig. 7(a), one can see the condensation with respect to temperature

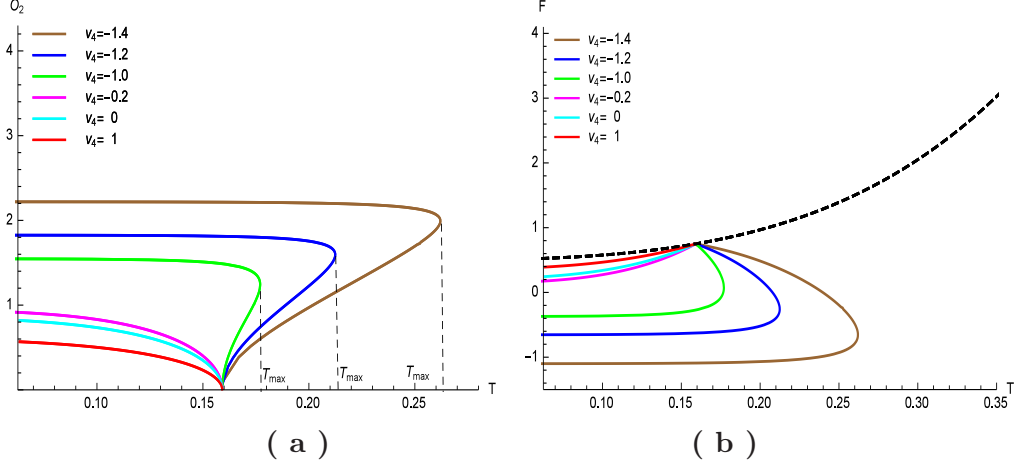


Figure 6. The condensation is as a function of temperature in massive scalar case with potential $V(\phi) = -\frac{12}{L^2} - \frac{16\phi^2}{3L^2} + \frac{\nu_4\phi^4}{L^2}$.

with choosing different values of coupling constant ν_6 . With increasing $\nu_6 = 0.0, 2.0$, the condensation will monotonically decrease from positive finite value to vanishing. In $\nu_6 < 0.0$ region, the condensation is multiple valued function of temperature as shown in Fig. 7(a) and there is a local maximal temperature T_{max} and minimal temperature T_{min} in each curve. For $\nu_6 = -0.1$, the condensation will decrease from $T = 0$ to $T = T_{min}$ and it will jump to less finite positive value at T_{min} . From $T_{min} < T < T_{max}$, the condensation will become multivalued function of temperature. For $T \geq T_{max}$, the condensation will decrease to zero continuously in Fig. 7(a). In Fig. 7(b), we have shown various free energy with respect to temperature with gradually changing the ν_6 . We also find that free energy with $\nu_6 = 0, 2$ is monotonically increasing with temperature. They always continuously converge to the transition point T_c . The transition point is defined by vanishing of condensation. But in cases with $\nu_6 = -0.1$, the free energy is multiple valued function of temperature. For these cases, there are minimal temperatures T_{mini} and local maximal temperature T_{max} . For $T > T_c$, hyperbolic AdS-SW black hole should be stable and there is no massive scalar hair black hole solution. In $T_{max} < T < T_c$ and $0 < T < T_{min}$, massive scalar hair black hole is more stable than hyperbolic AdS-SW black hole. In $T_{min} < T < T_{max}$, the condensation of dual operator is a multiple valued function and the stable solution is marked by solid curve in Fig. 7(a)(b) in terms of comparing free energy. There is critical value ν_{6c} such that $T_{min} = T_{max}$. Therefore, there are two types of phase transitions for $\nu_6 = -0.5$. The first one happens at T_{max} and the condensation is not continuous function of temperature at T_{max} with $\nu_6 < \nu_{6c}$. The other one happens at T_c and condensation goes to zero with $\nu_6 > \nu_{6c}$.

In the third case, we will focus on the condensation with potential $V(\phi) = -\frac{12}{L^2} - \frac{16\phi^2}{3L^2} + \frac{\nu_3\phi^3}{L^2}$. In Fig. 8(a), we can find that the condensation will decrease from positive finite value to vanishing in $\nu_3 > \nu_{3c}$ region. In our setup, $\nu_{3c} = 0$. In $\nu_3 < 0$ region, the condensation will be multiple valued function of temperature. This case is much similar to first massive

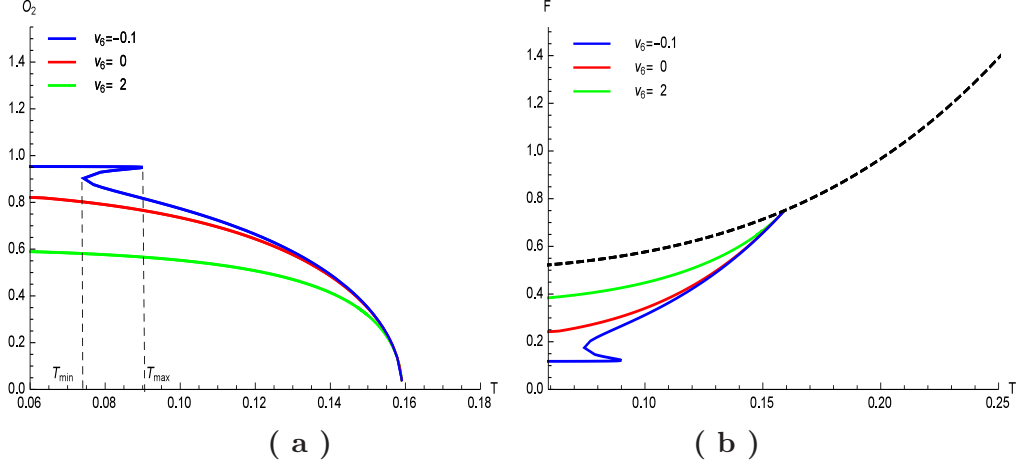


Figure 7. The condensation O is as a function of temperature T in massive scalar case with potential $V(\phi) = -\frac{12}{L^2} - \frac{16\phi^2}{3L^2} + \frac{\nu_6\phi^6}{L^2}$.

case. In this region, the transition order will be change. Because the condensation can not continuously decrease to zero at transition temperature and it will suddenly jump from positive finite value to zero. In 8(b), we have shown the free energy as function of temperature. In $\nu_3 > 0$ region, free energy is monotonically increasing with temperature, while free energy is multiple valued function of temperature in $\nu_3 < 0$. That means the free energy can not converge to the transition temperature continuously, while massive hair black hole will jump to hyperbolic AdS-SW black hole at transition temperature. Roughly speaking, the phase transitions induced by $\frac{\nu_3\phi^3}{L^2}$ is almost similar to ones induced by $\frac{\nu_4\phi^4}{L^2}$.

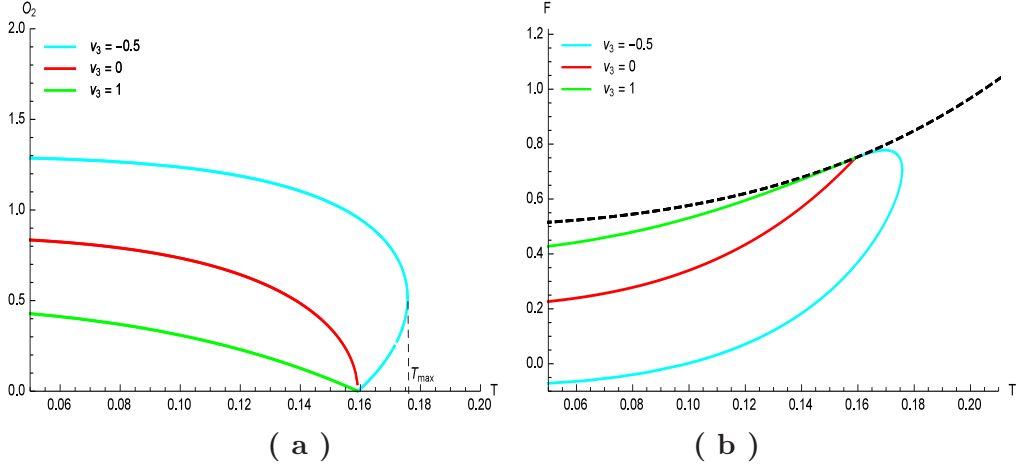


Figure 8. The condensation O is as a function of temperature T in massive scalar case with potential $V(\phi) = -\frac{12}{L^2} - \frac{16\phi^2}{3L^2} + \frac{\nu_3\phi^3}{L^2}$.

Finally, we would like to focus on the condensation in massive scalar with potential $V(\phi) = -\frac{12}{L^2} - \frac{16\phi^2}{3L^2} + \frac{\nu_4\phi^4}{L^2} + \frac{\nu_6\phi^6}{L^2}$. The main motivation to study this case is that we expect to

find competitive mechanism between $\frac{\nu_4\phi^4}{L^2}$ deformation and $\frac{\nu_6\phi^6}{L^2}$ deformation. In Fig. 9(a), one can vary ν_6 with fixing $\nu_4 = 1.0$ to see that the condensation will monotonically decrease to zero from low temperature to high temperature for $\nu_6 > \nu_{6c}$. In $\nu_4 = 1$ case, $\nu_{6c} = 0.0$ such that $T_{min} = T_{max}$. For fixing ν_4 , one can tune $\nu_6 = \nu_{6c}$ to be a solution in which T_{max} will coincide with T_{min} . One can vary ν_4 to find corresponding ν_{6c} . While in Fig. 9(b), we confirm that the hairy black hole solution is much stable than hyperbolic AdS-SW in $T_{max} < T < T_c$ and $0 < T < T_{min}$ with $\nu_6 < \nu_{6c}, \nu_4 = 1$. Where T_c is defined by the point where the condensation is vanishing in Fig. 9(a) and T_{min}, T_{max} are marked in Fig. 9(a). In $T > T_c$, there is no stable hairy black hole solution for $\nu_6 > \nu_{6c}$ and hyperbolic AdS-SW solution is stable one. In $\nu_6 < \nu_{6c}$, the condensation will become multivalued function of temperature from $T_{min} < T < T_{max}$. For $\nu_6 = -0.5$ example, the stable configuration in $0 < T < T_{min}$ is the hairy black hole solution, while in $T > T_c > T_{min}$ is hyperbolic AdS-SW black solution. When $T_{min} < T < T_c < T_{max}$ as shown in Fig. 9, there is a phase transition between two hairy AdS black holes and the condensation will jump from positive finite value to less positive finite value. Especially at T_c , there is phase transition between hairy black hole and hyperbolic AdS-SW black hole due to condensation goes to vanishing. These numerical studies show that there is competitive mechanism between $\frac{\nu_4\phi^4}{L^2}$ deformation and $\frac{\nu_6\phi^6}{L^2}$ deformation. One can tune ν_4, ν_6 to see which phase is stable and what type of phase transition happens. One can set $\nu_4 = 0$ and this numerical result will reproduce one in second massive case.

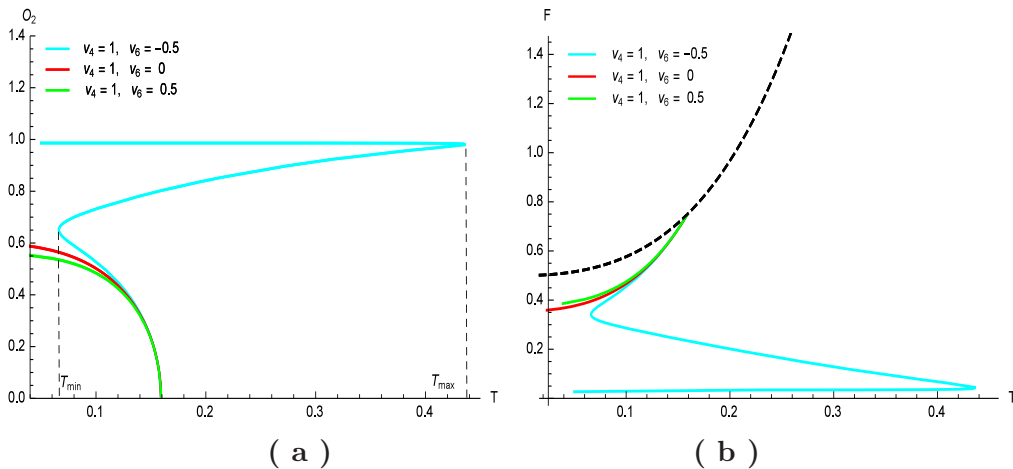


Figure 9. The condensation O is as a function of temperature T in massive scalar case with potential $V(\phi) = -\frac{12}{L^2} - \frac{16\phi^2}{3L^2} + \frac{\nu_4\phi^4}{L^2} + \frac{\nu_6\phi^6}{L^2}$.

To close this subsection, we would like to give a short summary. Here we have introduced various deformations in massive scalar potential and study these deformations effects on stability of hairy AdS hyperbolic black holes case by case. In each case, the condensation as a function of temperature implies that there exist phase transitions in deformed theories. The behavior of condensation and free energy with respect to temperature in ϕ^3 and ϕ^4 deformed theories will be similar to ones in the massless cases with ϕ^3, ϕ^4, ϕ^6

deformation. Comparing with Fig.10 Fig.11 Fig.12, it has exotic behavior with respect to temperature in ϕ^6 deformed theories shown in Fig.7 Fig.9. The exotic behavior is induced by ϕ^6 deformation essentially. All these behaviors imply that there may exist phase transitions. Essentially, all these phase transitions mainly originate from the effective mass of scalar below the effective BF bound for the near horizon AdS_2 . However, it is not enough to confirm the phase transitions by analyzing the condensation of dual operator and free energy. In section 7, we will see the hyperbolic hairy AdS black hole solutions will be stable in low temperature region $T < T_c$ when coupling constants live in specific regions. Otherwise, these solutions will not be stable anymore and there exist much more stabler in-homogenous solutions. We will see details in section 7.

7 Instability for the Normalizable Mode

Previous discussions on the stability of different phases are mainly based on thermodynamical analysis with comparing free energy. Comparing free energy between constant solution and hyperbolic AdS-SW is not enough to make sure these new hyperbolic solutions are stable or not. To be more rigorous, in this section we will investigate the instability of these solutions under scalar perturbation $\delta\Phi(t, z, \psi, \theta, \varphi)$. The wave function of $\delta\Phi(t, z, \psi, \theta, \varphi)$ could be decomposed as

$$\delta\Phi(t, z, \psi, \theta, \varphi) = e^{\omega t} \delta\phi(z) Y(\psi, \theta, \varphi), \nabla_{\mathbf{H}_3}^2 Y(\psi, \theta, \varphi) = -\lambda Y(\psi, \theta, \varphi), \quad (7.1)$$

with Y the eigenfunction of Laplacian in certain manifold Σ and λ the corresponding eigenvalues. When Σ is just the hyperboloid H_{d-2} , λ has the lower bound $\lambda > \frac{(d-3)^2}{4}$. Here, we will consider the 5D case, so $d = 5$ and $\lambda > 1$. More generally, when Σ is a non-trivial quotient of hyperboloid, then the lower bound of λ would be extended to 0. Thus, below we will only consider $\lambda > 0$ and $\omega^2(\lambda = 0)$ for simplicity [18] [19].

Under the ansatz Eq.(7.1), the equation of motion for $\delta\phi$ could be derived as follows

$$\delta\phi'' + \left(-\frac{3}{z} + 3A'_e + \frac{f'}{f}\right)\delta\phi' + \left(\frac{3e^{2A_e}}{8z^2 f} V''(\phi) - \frac{\omega^2}{f^2} + \frac{\lambda}{f}\right)\delta\phi = 0, \quad (7.2)$$

where A_e, f, ϕ are associated with background solutions. In our ansatz Eq.(7.1), the time related part behaves as $e^{\omega t}$. The black hole will be unstable if (7.2) has a solution with real and positive ω^2 with the field satisfying specific boundary conditions at infinity and the horizon. Therefore, if there exist solutions with positive ω^2 in certain background solutions, then the background solutions are unstable. This instability is induced by inhomogenous perturbation in boundary special direction. If one can not find such perturbative modes with positive ω^2 , then the background solutions are stable at the level of linear perturbation. This is the key criterion to test the stability of these solutions. In principle, one should construct hairy black holes at the non-linear level which is considerably more difficult. In this paper, it is sufficient to demonstrate that an instability exists by linear perturbation.

The leading expansion of $\delta\phi$ near the horizon $z = z_h$ could be derived from Eq.(7.2) as following

$$\delta\phi(z) = \delta p_{h1}(z_h - z)^{\frac{\omega}{4\pi T}}(1 + \dots) + \delta p_{h2}(z_h - z)^{-\frac{\omega}{4\pi T}}(1 + \dots), \quad (7.3)$$

with $\delta p_1, \delta p_2$ the two integral constants of the second order derivative equation Eq.(7.2). Without loss of generality, we assume $\omega = \sqrt{\omega^2} > 0$, then the δp_{h1} mode tends to 0 when z approaches z_h , while the δp_{h2} mode is divergent near horizon. Thus, the near horizon boundary condition is easy to be set as $\delta\phi(z_h) = 0$.

For the UV boundary condition, again, we could calculate the near boundary expansion of $\delta\phi$ from Eq.(7.2). It depends on the dimension of ϕ . For $\Delta = 2$ as example, the leading expansion is of the form

$$\delta\phi(z) = \delta p_{01}^2 z^2 \log(z) + \dots + \delta p_{02}^{(2)} z^2 + \dots \quad (7.4)$$

As in the background solutions, we will require the coefficient of $z^2 \log(z)$ to be 0. For $\Delta = 4$, one can obtain the UV boundary condition as

$$\delta\phi(z) = \delta p_0^{(0)} + \delta p_0^{(4)} z^4 + \dots \quad (7.5)$$

In general, only for certain groups of (λ, ω^2) the solutions of $\delta\phi$ could satisfy both the UV and IR boundary conditions simultaneously. We will try to find such kind of solutions under the background solutions solved in previous sections, and to see whether it is stable or not under the linear perturbation.

7.1 Massless Scalar Cases

Firstly, we focus on the stability in the massless cases. In terms of previous arguments in last section, one just only studies the sign of $\omega^2(\lambda = 0)$ and we can test stability of these solutions solved in previous several sections.

In Fig.10 Fig.11 Fig.12, we show the $\omega^2(\lambda = 0)$ as a function of temperature numerically with turning on the linear perturbation of hyperbolic black hole solution with $V(\phi) = -\frac{12}{L^2} + \frac{\nu_4\phi^4}{L^2}$, $V(\phi) = -\frac{12}{L^2} + \frac{\nu_4\phi^4}{L^2} + \frac{\nu_6\phi^6}{L^2}$ and $V(\phi) = -\frac{12}{L^2} + \frac{\nu_3\phi^3}{L^2} + \frac{\nu_4\phi^4}{L^2}$ respectively. In all these cases, one can see that $\omega^2(\lambda = 0)$ always positive from low to high temperature region. These solutions shown in Fig.3 Fig.4 Fig.5 should be unstable configurations, although these configurations are much more stable than hyperbolic AdS-SW black hole with comparing free energy. One can see that there should exist in-homogenous black hole solutions which break the hyperbolic symmetry.

7.2 Massive Scalar Cases

In this subsection, we turn to focus on the stability of new hyperbolic black hole solutions with massive scalar potentials. Here we have studied four cases which are shown in Fig.13 Fig.14 Fig.15 Fig.16. Here we summarize final results in the following. In Fig.13 Fig.14 Fig.15 Fig.16, we show the $\omega^2(\lambda = 0)$ as a function of temperature numerically with turning on the linear perturbation of hyperbolic black hole solution with $V(\phi) = -\frac{12}{L^2} - \frac{16\phi^2}{3L^2} + \frac{\nu_4\phi^4}{L^2}$, $V(\phi) = -\frac{12}{L^2} - \frac{16\phi^2}{3L^2} + \frac{\nu_6\phi^6}{L^2}$, $V(\phi) = -\frac{12}{L^2} - \frac{16\phi^2}{3L^2} + \frac{\nu_3\phi^3}{L^2}$ and $V(\phi) = -\frac{12}{L^2} - \frac{16\phi^2}{3L^2} + \frac{\nu_4\phi^4}{L^2} + \frac{\nu_6\phi^6}{L^2}$

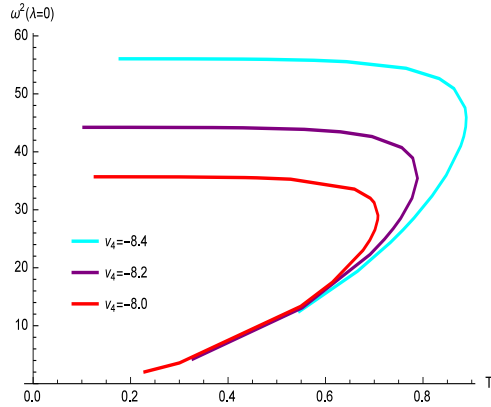


Figure 10. $\omega^2(\lambda = 0)$ as a function of temperature in massless scalar case with potential $V(\phi) = -\frac{12}{L^2} + \frac{\nu_4 \phi^4}{L^2}$ at the same parameter values as in Fig.3.

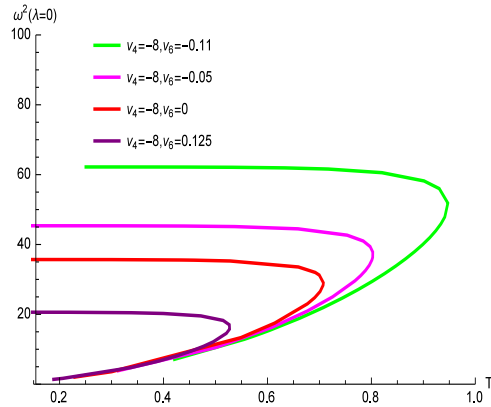


Figure 11. $\omega^2(\lambda = 0)$ as a function of temperature in massless scalar case with potential $V(\phi) = -\frac{12}{L^2} + \frac{\nu_4 \phi^4}{L^2} + \frac{\nu_6 \phi^6}{L^2}$ at the same parameter values as in Fig.4.

respectively. For massive scalar cases, there are something new presented. Up to linear perturbative analysis, some solutions are stable. For example, as shown in Fig.13, we can tune v_4 gradually and then we can find a critical value of $v_4 = 0$. Once $v_4 > 0$, $\omega^2(\lambda = 0)$ are always negative definite function of temperature and which also means $v_4 > 0$ these solutions found in Fig.6 might be stable at level of linear perturbation analysis. The phase transition shown in Fig.14 might truly happen. Such kind of phenomenon also happens in Fig.14. One can also tune the v_6 gradually to find the critical value of $v_6 = 0$. When v_6 becomes positive, one can not find positive definite $\omega^2(\lambda = 0)$ which implies that solutions with positive v_6 might be also stable and phase transition might happen in Fig.7. In Fig.15, one can also tune the v_3 gradually to find critical value $v_3 = 0$ and similar story will happen as shown in Fig.13 Fig.14. Finally, we consider more complicated situation with potential $V(\phi) = -\frac{12}{L^2} - \frac{16\phi^2}{3L^2} + \frac{\nu_4 \phi^4}{L^2} + \frac{\nu_6 \phi^6}{L^2}$. For simplifying our study, we just fix $v_4 = 1$ and gradually

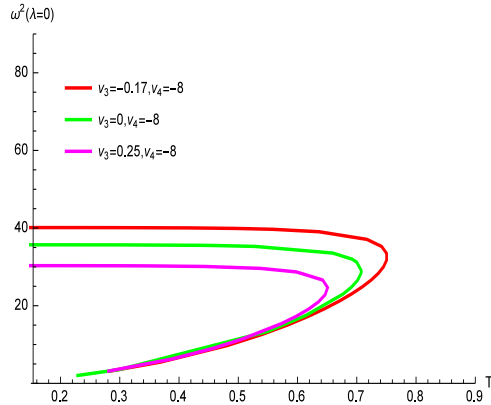


Figure 12. $\omega^2(\lambda = 0)$ as a function of temperature in massless scalar case with potential $V(\phi) = -\frac{12}{L^2} + \frac{\nu_3\phi^3}{L^2} + \frac{\nu_4\phi^4}{L^2}$ at the same parameter values as in Fig.5.

tune v_6 to obtain the critical value $v_6 = 0$ such that there is no positive $\omega^2(\lambda = 0)$ existing in the black hole solution. We expect that the solutions found in Fig.9 with positive v_6 are stable and the phase transition might really happen.

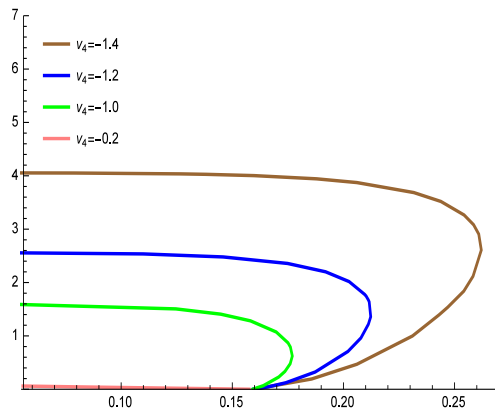


Figure 13. $\omega^2(\lambda = 0)$ as a function of temperature in massive scalar case with potential $V(\phi) = -\frac{12}{L^2} - \frac{16\phi^2}{3L^2} + \frac{\nu_4\phi^4}{L^2}$ at the same parameter values as in Fig.6. When $v_4 = 0, 1$, we did not find positive ω^2 at $\lambda = 0$.

8 Comments on Renyi Entropy in CFTs

In this section, we would like to connect the instability of hyperbolic AdS black hole with holographic Renyi Entropy. Before we comment on this connection, we would like to brief review the replica trick in various aspects as a starting point of this section. In the recent literature, many progresses of calculation of Renyi Entropy have been achieved. Especially, Renyi entropy of a spherical entangling surface in field theories can be evaluated

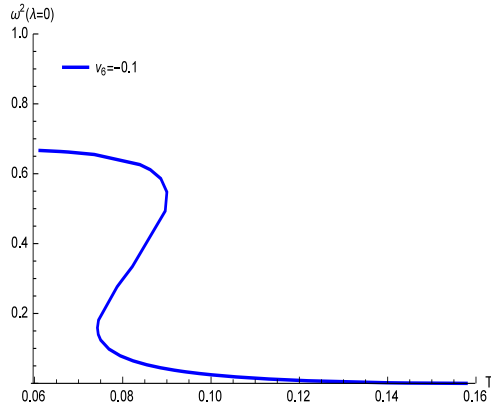


Figure 14. $\omega^2(\lambda = 0)$ as a function of temperature in massive scalar case with potential $V(\phi) = -\frac{12}{L^2} - \frac{16\phi^2}{3L^2} + \frac{\nu_6\phi^6}{L^2}$ at the same parameter values as in Fig.7. When $v_6 = 0, 2$, we did not find positive ω^2 at $\lambda = 0$.

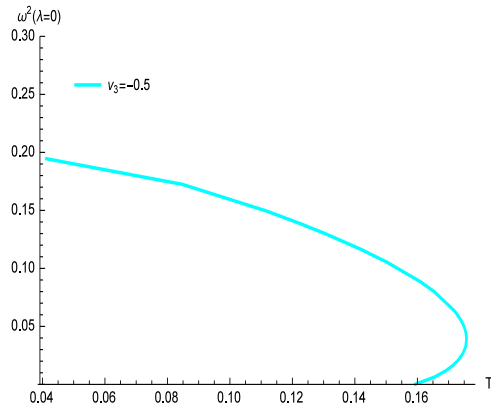


Figure 15. $\omega^2(\lambda = 0)$ as a function of temperature in massive scalar case with potential $V(\phi) = -\frac{12}{L^2} - \frac{16\phi^2}{3L^2} + \frac{\nu_3\phi^3}{L^2}$ at the same parameter values as in Fig.8. When $v_3 = 0, 1$, we did not find positive ω^2 at $\lambda = 0$.

the thermal entropy on dual hyperbolic AdS black holes. Finally, we comment on how the instability of hyperbolic AdS black holes will induce a phase transition in dual field theory by holographic Renyi Entropy.

8.1 Replica and Renyi Entropy

Entanglement entropy (EE) and the entanglement Rényi entropy (ERE) are very helpful quantities to study phase transitions in QFTs. The standard approach to calculate entanglement entropy in field theory is called replica trick [32][33][34]. Recently, this approach has been widely used in field theory and holography[35][36][37][38]. The ERE for vacuum in various situations [39][40][41][43][44] has been studied. More recently, the ERE for local excited states in CFTs have been extensively investigated in [45][46] [47][48][50][51][52]. In

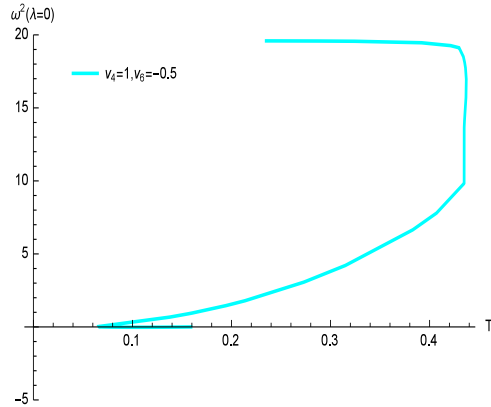


Figure 16. $\omega^2(\lambda = 0)$ as a function of temperature in massive scalar case with potential $V(\phi) = -\frac{12}{L^2} - \frac{16\phi^2}{3L^2} + \frac{\nu_4\phi^4}{L^2} + \frac{\nu_6\phi^6}{L^2}$ at the same parameter values as in Fig.9. When $v_6 = 0, 0.5$, we did not find positive ω^2 at $\lambda = 0$.

string theory, [53] tried to use replica trick to calculate entanglement entropy associated to black hole entropy in string theory.

In holography, the replica approach should start with calculating the partition function on n -fold cover of the background geometry. If one want to construct the structure for boundary CFT in terms of holography, it is inevitable to produce a conical singularity in the bulk. It is hard to resolve the bulk singularity without completely understanding the string theory or quantum gravity in the AdS bulk. In [54][55], authors have given a preliminary derivation of holographic Renyi entropy and [56] clarify this construction and extend this to more general spherical entangling surfaces in boundary CFT which is put on $R \times S^{d-1}$. These pioneer studies allow us to calculate the Renyi entropy of a spherical entangling surface by evaluating the thermal entropy on the hyperbolic cylinder $R \times H^{d-1}$. The essential new ingredient is that we should know hyperbolic AdS black hole solutions. Applying this approach, there are many extending studies [57][20][58].

8.2 Spherical Renyi Entropy as Thermal Entropy

A holographic calculation of Renyi entropy for a spherical entangling surface is derived in [56][54][55]. Following the this construction, the density matrix is thermal and we can write the q 'th power of ρ as following

$$\rho^q = U^{-1} \frac{\exp[-qH/T_0]}{Z(T_0)^q} U \quad \text{where} \quad Z(T_0) \equiv \text{tr} \left[e^{-H/T_0} \right]. \quad (8.1)$$

where q is integer number. The unitary transformation U and its inverse will be canceled with taking the trace of this expression. Hence the trace of q th power of density matrix is

$$\text{tr} [\rho^q] = \frac{Z(T_0/q)}{Z(T_0)^q}. \quad (8.2)$$

With using the definition of the free energy of dual black hole, i.e. $F(T) = -T \log Z(T)$, the corresponding Rényi entropy becomes

$$S_q = \frac{q}{(1-q)T_0} (F(T_0) - F(T_0/q)). \quad (8.3)$$

in terms of derivation[56][54][55]. Further using $S = -\partial F/\partial T$, this expression can be rewritten as

$$S_q = \frac{q}{q-1} \frac{1}{T_0} \int_{T_0/q}^{T_0} S_{\text{therm}}(T) dT, \quad (8.4)$$

where S_q is the Rényi entropy while $S_{\text{therm}}(T)$ denotes the thermal entropy of the CFT on $R \times H^{d-1}$. The entanglement entropy can be

$$S_{\text{EE}} = \lim_{q \rightarrow 1} S_q = S_{\text{therm}}(T_0). \quad (8.5)$$

with T_0 given by $\frac{1}{2\pi R}$. R is the curvature scale on the hyperbolic spatial slices H^{d-1} matching the radius of the original spherical entangle surface, R .

We can compute the Rényi entropy from these thermal entropies, via (8.4)

$$S_n = \frac{n}{n-1} \frac{1}{T_0} \left(\int_{T_0/n}^{T_{\text{cri}}} S_{\text{therm}}^{Eh}(T) dT + \int_{T_{\text{cri}}}^{T_0} S_{\text{therm}}^E(T) dT \right), \quad (8.6)$$

where $S_{\text{therm}}^{Eh}(T)$ is the entropy of the hairy black hole and $S_{\text{therm}}^E(T)$ is the entropy of the Einstein black hole. In terms of above formula, the Rényi entropy as a function of n . Because the derivative of the thermal entropy with respect to the temperature is discontinuous, the second derivative with respect to n of the Rényi entropy is discontinuous. Such kind of discontinuous is closely related to instability of hyperbolic AdS black hole. Such instability has been carefully studied in section 6 and section 7. Therefore, the discontinuous of Rényi entropy implies a phase transition in dual field theory by holography. In order to determine the precise value of n_c at which this transition occurs, one should study numerically the scalar wave equation within the black hole background as shown in [57][20]. The critical temperature is defined by $T_{\text{cri}} = \frac{1}{2n_c\pi R}$. Up to now, we completely get the hairy hyperbolic AdS black holes. Due to presence of condensation dual to scalar, the conformal transformation will break down in the whole background and one may not identify the Rényi entropy as the thermal entropy of hyperbolic AdS black hole generally. However, one can perturbatively extract Rényi entropy near transition point from hyperbolic AdS-SW black hole to hairy hyperbolic AdS black holes. Our studies will give us some insights on the Rényi entropy in dual field theory.

9 Conclusions and Discussions

In this paper, we have constructed various new hyperbolic asymptotic AdS gravity solutions in ED system numerically. Motivated by studying ERE with spherical entangling surface in deformed CFTs, we work out the background with introducing series powers of neutral

scalar in scalar potential. In this paper, we just focus on potential with ϕ^3, ϕ^4, ϕ^6 or some superpositions of them. Especially, we only focus on two kinds of special scalar potentials. The one is massless scalar with higher powers of scalar self interaction and the other is that we choose square of the scalar mass to be -3 . In terms of AdS/CFT, the first kind of scalar corresponds to gluon sector in gauge field theory side and the other scalar is dual to chiral condensation in field theory side. In general, to calculate the ERE with complicated entanglement surface is very hard. For spherical entanglement surface, one can make use of proposals [56][54][55] to relate the ERE to the thermal entropy in hyperbolic space. That means once you know the hyperbolic asymptotic AdS solutions, you can obtain the ERE with spherical entangling surface in dual CFTs. We have shown the configuration of these new hyperbolic AdS solutions and also extract the condensation of operators which dual to massless and massive scalars respectively. Through studying condensation with respect to temperature, they give us insight that there exist phase transitions. We list the well defined boundary energy momentum tensor by introducing proper boundary counter terms in each solution. With these counter terms, the finite free energy can be achieved. We just compare free energy between the new hyperbolic AdS solutions and hyperbolic AdS-SW solution to check the stability of these solutions. And then, to be more rigid, we turn on in-homogenous perturbation on these new hyperbolic AdS black holes to study the stability. We tune the potential parameters to figure out the stable region for potential parameters in these solutions, for example, the coefficients of the cubic, quartic and sextic scalar interactions v_3, v_4, v_6 . For massless scalar cases, we can not find stable solutions with turning on ϕ^3, ϕ^4, ϕ^6 in scalar potential respectively. Therefore, we can not safely say phase transition shown in Fig.3 Fig.4 Fig.5 really happens. There must exist stable solution with in-homogenous structure. For massive scalar cases with positive potential parameters v_3, v_4, v_6 respectively, ϕ^3, ϕ^4 will induce similar phase transition qualitatively shown in Fig.6 Fig.8, while ϕ^6 term in scalar potential will induce different kind phase transition in Fig.7. If one turns on superposition of ϕ^3, ϕ^4 and ϕ^6 in scalar potential, there exists competitive mechanism between phase transitions induced by ϕ^3, ϕ^4 and ϕ^6 in Fig.9. However, when we choose negative potential parameters v_3, v_4, v_6 respectively, our studies show that all these black hole solutions are not stable ones. With negative potential parameters v_3, v_4, v_6 , there may exist in-homogenous solutions which much more stable than corresponding hyperbolic AdS black hole solutions. Finally, the ERE can also be obtained in terms of proposals [56][54][55]. Further, we comment on ERE also implies phase transitions which has something do with instability of these new hyperbolic AdS solutions. Once we know the phase structures of various black hole solutions, we make use of [56][54][55] to comment on the spherical entanglement entropy in the dual field theory. In this sense, the stability of these black hole solutions is closely related to the spherical ERE in holographic dual CFTs and it gives some insight of phase transitions in dual field theory.

In this paper, we just focus on massless and massive scalar cases with higher powers of self interaction in potentials. In general, such kinds of deformation will lead to various types of phase transitions which are highly sensitive to the operators chosen and types of deformations. ERE can be also regarded as an order parameter to give some insight on

phase transitions in dual field theories.

Acknowledgements

We are grateful to Janet Hung, Li Li, S. Matsuura, Tadashi Takayanagi and Stefan Theisen for very useful conversations and correspondences. Z.F. and D.L. thank Yue-Liang Wu for his supports. S.H. thanks Ronggen Cai, Tadashi Takayanagi, Stefan Theisen for their encouragements and supports. S.H. is supported by Max-Planck fellowship and by the National Natural Science Foundation of China (No.11305235). D.L. is supported by China Postdoctoral Science Foundation.

References

- [1] J. M. Maldacena, “The large N limit of superconformal field theories and supergravity,” *Adv. Theor. Math. Phys.* **2**, 231 (1998) [*Int. J. Theor. Phys.* **38**, 1113 (1999)] [arXiv:hep-th/9711200].
- [2] S. S. Gubser, I. R. Klebanov and A. M. Polyakov, “Gauge theory correlators from non-critical string theory,” *Phys. Lett. B* **428**, 105 (1998) [arXiv:hep-th/9802109].
- [3] E. Witten, “Anti-de Sitter space and holography,” *Adv. Theor. Math. Phys.* **2**, 253 (1998) [arXiv:hep-th/9802150].
- [4] O. Aharony, S. S. Gubser, J. M. Maldacena, H. Ooguri and Y. Oz, “Large N field theories, string theory and gravity,” *Phys. Rept.* **323**, 183 (2000) [arXiv:hep-th/9905111].
- [5] S. A. Hartnoll, C. P. Herzog and G. T. Horowitz, “Building a Holographic Superconductor,” *Phys. Rev. Lett.* **101**, 031601 (2008) doi:10.1103/PhysRevLett.101.031601 [arXiv:0803.3295 [hep-th]].
- [6] S. A. Hartnoll, C. P. Herzog and G. T. Horowitz, “Holographic Superconductors,” *JHEP* **0812**, 015 (2008) doi:10.1088/1126-6708/2008/12/015 [arXiv:0810.1563 [hep-th]].
- [7] S. Aminneborg, I. Bengtsson, S. Holst and P. Peldan, “Making anti-de Sitter black holes,” *Class. Quant. Grav.* **13**, 2707 (1996) doi:10.1088/0264-9381/13/10/010 [gr-qc/9604005].
- [8] R. B. Mann, “Pair production of topological anti-de Sitter black holes,” *Class. Quant. Grav.* **14**, L109 (1997) doi:10.1088/0264-9381/14/5/007 [gr-qc/9607071].
- [9] R. B. Mann, “Charged topological black hole pair creation,” *Nucl. Phys. B* **516**, 357 (1998) doi:10.1016/S0550-3213(97)00833-X [hep-th/9705223].
- [10] R. Emparan, “AdS / CFT duals of topological black holes and the entropy of zero energy states,” *JHEP* **9906**, 036 (1999) doi:10.1088/1126-6708/1999/06/036 [hep-th/9906040].
- [11] R. Emparan, “AdS membranes wrapped on surfaces of arbitrary genus,” *Phys. Lett. B* **432**, 74 (1998) doi:10.1016/S0370-2693(98)00625-X [hep-th/9804031].
- [12] D. Birmingham, “Topological black holes in Anti-de Sitter space,” *Class. Quant. Grav.* **16**, 1197 (1999) doi:10.1088/0264-9381/16/4/009 [hep-th/9808032].
- [13] O. J. C. Dias, R. Monteiro, H. S. Reall and J. E. Santos, “A Scalar field condensation instability of rotating anti-de Sitter black holes,” *JHEP* **1011**, 036 (2010) doi:10.1007/JHEP11(2010)036 [arXiv:1007.3745 [hep-th]].

- [14] I. Robinson, *Bull. Acad. Pol. Sci. Ser. Sci. Math. Astron. Phys.* **7** (1959) 351.
- [15] B. Bertotti, *Phys. Rev.* **116** (1959) 1331.
- [16] J. M. Bardeen and G. T. Horowitz, “The Extreme Kerr throat geometry: A Vacuum analog of AdS(2) x S**2,” *Phys. Rev. D* **60**, 104030 (1999) doi:10.1103/PhysRevD.60.104030 [hep-th/9905099].
- [17] Y. Brihaye and B. Hartmann, “Stability of Gauss-Bonnet black holes in Anti-de-Sitter space-time against scalar field condensation,” *Phys. Rev. D* **84**, 084008 (2011) doi:10.1103/PhysRevD.84.084008 [arXiv:1107.3384 [gr-qc]].
- [18] A. Belin and A. Maloney, “A New Instability of the Topological black hole,” arXiv:1412.0280 [hep-th].
- [19] A. Belin, A. Maloney and S. Matsuura, “Holographic Phases of Renyi Entropies,” *JHEP* **1312**, 050 (2013) [arXiv:1306.2640 [hep-th]].
- [20] A. Belin, L. Y. Hung, A. Maloney and S. Matsuura, “Charged Renyi entropies and holographic superconductors,” *JHEP* **1501**, 059 (2015) [arXiv:1407.5630 [hep-th]].
- [21] S. He, D. Li and J. B. Wu, “Entanglement Temperature in Non-conformal Cases,” *JHEP* **1310**, 142 (2013) doi:10.1007/JHEP10(2013)142 [arXiv:1308.0819 [hep-th]].
- [22] M. Henningson and K. Skenderis, “The Holographic Weyl anomaly,” *JHEP* **9807**, 023 (1998) [hep-th/9806087].
- [23] M. Henningson and K. Skenderis, “Holography and the Weyl anomaly,” *Fortsch. Phys.* **48**, 125 (2000) [hep-th/9812032].
- [24] V. Balasubramanian and P. Kraus, “A Stress tensor for Anti-de Sitter gravity,” *Commun. Math. Phys.* **208**, 413 (1999) [hep-th/9902121].
- [25] S. Hyun, W. T. Kim and J. Lee, “Statistical entropy and AdS / CFT correspondence in BTZ black holes,” *Phys. Rev. D* **59**, 084020 (1999) [hep-th/9811005].
- [26] R. Emparan, C. V. Johnson and R. C. Myers, “Surface terms as counterterms in the AdS / CFT correspondence,” *Phys. Rev. D* **60**, 104001 (1999) [hep-th/9903238].
- [27] R. B. Mann, “Misner string entropy,” *Phys. Rev. D* **60**, 104047 (1999) doi:10.1103/PhysRevD.60.104047 [hep-th/9903229].
- [28] K. Skenderis, “Lecture notes on holographic renormalization,” *Class. Quant. Grav.* **19**, 5849 (2002) [hep-th/0209067].
- [29] S. de Haro, S. N. Solodukhin and K. Skenderis, “Holographic reconstruction of space-time and renormalization in the AdS / CFT correspondence,” *Commun. Math. Phys.* **217**, 595 (2001) [hep-th/0002230].
- [30] S. Nojiri and S. D. Odintsov, “Conformal anomaly for dilaton coupled theories from AdS / CFT correspondence,” *Phys. Lett. B* **444**, 92 (1998) doi:10.1016/S0370-2693(98)01351-3 [hep-th/9810008].
- [31] S. Nojiri, S. D. Odintsov and S. Ogushi, “Finite action in d-5 gauged supergravity and dilatonic conformal anomaly for dual quantum field theory,” *Phys. Rev. D* **62**, 124002 (2000) doi:10.1103/PhysRevD.62.124002 [hep-th/0001122].
- [32] C. G. Callan, Jr. and F. Wilczek, “On geometric entropy,” *Phys. Lett. B* **333**, 55 (1994) [hep-th/9401072].

- [33] P. Calabrese and J. L. Cardy, “Entanglement entropy and quantum field theory,” *J. Stat. Mech.* **0406**, P06002 (2004) [hep-th/0405152].
- [34] P. Calabrese and J. L. Cardy, “Entanglement entropy and quantum field theory: A Non-technical introduction,” *Int. J. Quant. Inf.* **4**, 429 (2006) [quant-ph/0505193].
- [35] S. Ryu and T. Takayanagi, “Holographic derivation of entanglement entropy from AdS/CFT,” *Phys. Rev. Lett.* **96**, 181602 (2006) doi:10.1103/PhysRevLett.96.181602 [hep-th/0603001].
- [36] S. Ryu and T. Takayanagi, “Aspects of Holographic Entanglement Entropy,” *JHEP* **0608**, 045 (2006) doi:10.1088/1126-6708/2006/08/045 [hep-th/0605073].
- [37] A. Lewkowycz and J. Maldacena, “Generalized gravitational entropy,” *JHEP* **1308**, 090 (2013) doi:10.1007/JHEP08(2013)090 [arXiv:1304.4926 [hep-th]].
- [38] W. Song, Q. Wen and J. Xu, “Generalized Gravitational Entropy for WAdS₃,” arXiv:1601.02634 [hep-th].
- [39] I. R. Klebanov, S. S. Pufu, S. Sachdev and B. R. Safdi, “Renyi Entropies for Free Field Theories,” *JHEP* **1204**, 074 (2012) [arXiv:1111.6290 [hep-th]].
- [40] T. Nishioka and I. Yaakov, “Supersymmetric Renyi Entropy,” *JHEP* **1310**, 155 (2013) [arXiv:1306.2958 [hep-th]].
- [41] C. A. Agon, M. Headrick, D. L. Jafferis and S. Kasko, “Disk entanglement entropy for a Maxwell field,” *Phys. Rev. D* **89**, no. 2, 025018 (2014) [arXiv:1310.4886 [hep-th]].
- [42] N. Hama, T. Nishioka and T. Ugajin, “Supersymmetric Renyi entropy in five dimensions,” *JHEP* **1412**, 048 (2014) [arXiv:1410.2206 [hep-th]].
- [43] X. Huang, S. J. Rey and Y. Zhou, “Three-dimensional SCFT on conic space as hologram of charged topological black hole,” *JHEP* **1403**, 127 (2014) [arXiv:1401.5421 [hep-th]].
- [44] N. Hama, T. Nishioka and T. Ugajin, “Supersymmetric Renyi entropy in five dimensions,” *JHEP* **1412**, 048 (2014) [arXiv:1410.2206 [hep-th]].
- [45] M. Nozaki, T. Numasawa and T. Takayanagi, “Quantum Entanglement of Local Operators in Conformal Field Theories,” *Phys. Rev. Lett.* **112**, 111602 (2014) [arXiv:1401.0539 [hep-th]].
- [46] M. Nozaki, “Notes on Quantum Entanglement of Local Operators,” *JHEP* **1410**, 147 (2014) [arXiv:1405.5875 [hep-th]].
- [47] S. He, T. Numasawa, T. Takayanagi and K. Watanabe, “Quantum Dimension as Entanglement Entropy in 2D CFTs,” *Phys. Rev. D* **90**, 041701 (2014) [arXiv:1403.0702 [hep-th]].
- [48] P. Caputa, M. Nozaki and T. Takayanagi, “Entanglement of local operators in large-N conformal field theories,” *PTEP* **2014**, 093B06 (2014) [arXiv:1405.5946 [hep-th]].
- [49] C. T. Asplund, A. Bernamonti, F. Galli and T. Hartman, “Holographic Entanglement Entropy from 2d CFT: Heavy States and Local Quenches,” *JHEP* **1502**, 171 (2015) [arXiv:1410.1392 [hep-th]].
- [50] W. Z. Guo and S. He, “Rényi entropy of locally excited states with thermal and boundary effect in 2D CFTs,” *JHEP* **1504**, 099 (2015) [arXiv:1501.00757 [hep-th]].
- [51] B. Chen, W. Z. Guo, S. He and J. q. Wu, “Entanglement Entropy for Descendent Local Operators in 2D CFTs,” arXiv:1507.01157 [hep-th].

- [52] M. Nozaki, T. Numasawa and S. Matsuura, “Quantum Entanglement of Fermionic Local Operators,” arXiv:1507.04352 [hep-th].
- [53] S. He, T. Numasawa, T. Takayanagi and K. Watanabe, “Notes on Entanglement Entropy in String Theory,” JHEP **1505**, 106 (2015) doi:10.1007/JHEP05(2015)106 [arXiv:1412.5606 [hep-th]].
- [54] R. C. Myers and A. Sinha, “Seeing a c-theorem with holography,” Phys. Rev. D **82**, 046006 (2010) [arXiv:1006.1263 [hep-th]].
- [55] R. C. Myers and A. Sinha, “Holographic c-theorems in arbitrary dimensions,” JHEP **1101**, 125 (2011) [arXiv:1011.5819 [hep-th]].
- [56] H. Casini, M. Huerta and R. C. Myers, “Towards a derivation of holographic entanglement entropy,” JHEP **1105**, 036 (2011) [arXiv:1102.0440 [hep-th]].
- [57] A. Belin, L. Y. Hung, A. Maloney, S. Matsuura, R. C. Myers and T. Sierens, “Holographic Charged Renyi Entropies,” JHEP **1312**, 059 (2013) [arXiv:1310.4180 [hep-th]].
- [58] A. R. Brown, D. A. Roberts, L. Susskind, B. Swingle and Y. Zhao, “Complexity Equals Action,” arXiv:1509.07876 [hep-th].